

Mechanochemical Problems of the Synthesis of Titanates

MARINA V. VLASOVA^{1,2}, JOSE G. GONZALEZ-RODRIGUEZ², MYKOLA G. KAKAZEY²,
ANDREY V. RAGULYA¹ and TAMARA V. TOMILA¹

¹*Institute for Problems of Materials Science, NAS of Ukraine,
Ul. Krzhizhanovskogo, 3, Kiev 03142 (Ukraine)*

E-mail: tomila@ipms.kiev.ua

²*Centro de Investigaciones en Ingenieria y Ciencias Aplicadas UAEM,
Cuernavaca, Mexico,*

E-mail: kakazey@hotmail.com

Abstract

An analysis of thermal processes occurring during mechanical treatment (MT) is presented. A two-stage scheme of development of thermal processes in ZnO, ZnO – TiO₂ systems is proposed and their role in the formation of the resulting defect structure is discussed. At the first stage of the MT, the collectivized processes of destruction of individual particles are observed. The second stage of processing is connected with the development of annealing effects caused by heat accumulation processes by the whole sample. The annealing processes favour the formation and accumulation of a set of associates of simple defects that accelerate diffusion processes in components of the mixtures. The processes of accumulation of associates of defects in the sample and a significant rise in the average temperature of the sample are major factors determining the progress of a mechanochemical reaction of the type $\text{ZnO} + \text{TiO}_2 \rightarrow \text{ZnTiO}_3$.

INTRODUCTION

Processes occurring during mechanical treatment (MT) are rather frequently considered within the framework of stationary external temperature conditions. Nevertheless, the situation is far from being unambiguous. It has been known that MT is accompanied by the development of thermal processes of different types [1–9]. The main areas of heat release during MT of disperse systems are zones of new surface formation, zones of dislocation development and displacement, and zones of interparticle friction (*i. e.* zones of active defect formation), zones of friction of the working parts of the reactor [1]. The formation of deformation-destruction zones is characterized by the appearance of high-temperature spikes (up to 1000 K) [3]. The crack propagation is accompanied by the formation of a short-lived ultrahigh temperature peak (up to 5000 K) [4, 6, 7]. This ultrahigh temperature

excitation lasts about 10^{-9} s [1]. During sliding friction, the temperature of contact areas increases up to the melting point of one of the substances [3, 5].

In the case when a single microcrack (or single dislocation zone) propagates, the shape of the ultrahigh temperature spike will depend only on the thermal conductivity of the material (Fig. 1, *a*). In the case when the destruction zone with high local density of microcracks forms, the transformation of a number of short-lived single ultrahigh-temperature spikes into an averaged “collective high-temperature spike” takes place (see Fig. 1, *b*). Such a spike has a significantly longer duration. The shape of the high temperature spike is determined by the thermal conduction of environment of the destruction zone. The combination of all local pulse mechanothermal processes leads to an increase of the average temperature, T_{av} , of the sample as a whole. In the case of prolonged MT, a certain time, t_{MT} ,

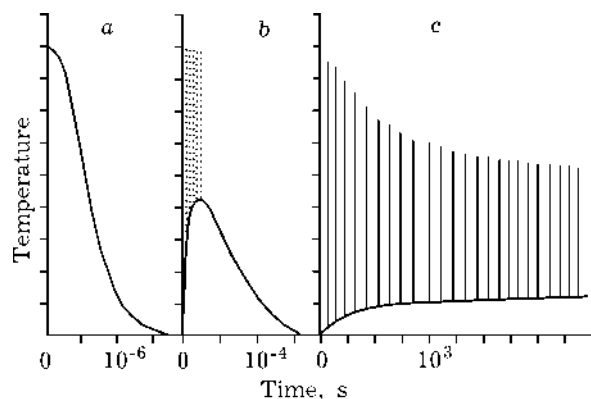


Fig. 1. Schemes of temperature kinetics during MT of disperse systems: *a* – at forming a single microcrack; *b* – in case of high local density of microcracks (contributions from single microcracks are indicated by the dashed lines); *c* – for the whole disperse system (thin vertical lines correspond to the contributions from “collective high-temperature spikes”).

is needed for the working system to go to the state of thermodynamic equilibrium with the environment. The kinetic scheme of the development of thermal processes in disperse system during MT, which takes into account collective processes, is presented in Fig. 1, *c*. Thus, particular defects formed during MT are subject to the thermal influence of both local ultrahigh temperature spike, collective high-temperature spikes, and the prolonged influence of the average temperature of the disperse system itself.

This report shows some possibilities of an experimental study by means of electron paramagnetic resonance (EPR) and IR spectroscopy of the role of the mechanothermal effects in the formation and evolution of defect structures in the ZnO – TiO₂ system during MT in a vibratory mill. It seems likely that it is just these processes that play the major role in proceeding interphase mechanochemical reaction of titanate formation (for instance, BaO + TiO₂ ® BaTiO₃ [10, 11] and ZnO + TiO₂ ® ZnTiO₃).

EXPERIMENTAL

We used to study powders of pure ZnO and a mixture of equal parts of ZnO and TiO₂ powders. TiO₂ and ZnO have specific surfaces $S_{sp} \gg 7 \text{ m}^2/\text{g}$ and $S_{sp} \gg 3.6 \text{ m}^2/\text{g}$, respectively. ZnO powder characteristics (obtained by dispersion analysis, EPR, IR-spectroscopy, elec-

tron microscopy, *etc.*) during mechanical treatment have been described elsewhere [12–14]. The samples under investigation can be considered as a mixture of powders in which individual ZnO particles are surrounded by particles of different materials (ZnO and TiO₂) of different thermal conductivity K ($\gg 17.5$ and $\gg 6.5 \text{ W}/(\text{m K})$, respectively) and microhardness H ($\gg 1500$ and $\gg 7800 \text{ MPa}$, respectively) [15]. MT of the powders was carried out in a vibratory mill (Tur MH 954/3 KXD HUMBOLDT NEDAG AG) in air for different times ranging from 0.5 to 300 min.

The EPR spectra were measured at room temperature with the X band radiospectrometer SE/X 2547-Radiopan connected with a spectrum analyzer and a PC.

The IR spectra of diluted samples (ZnO and ZnO + TiO₂ powders were mixed with KBr in ratio of 1 mg : 300 mg) were recorded with a Specord-M80 spectrometer. For this purpose, the obtained mixture was pressed into transparent rectangular plates with dimensions 5 × 26 mm. The theoretical approach to the calculation of an infrared spectrum of a powder composed of small particles includes the so-called theory of the average dielectric constant (TADC) [16]. In this theory, the particle shape is assumed to be a revolution ellipsoid that rotates around its own *c*-axis. The shapes of small particles as well as aggregation are considered from the viewpoint of depolarization effects taking into account the shape factors L_{\perp} and L_{\parallel} (where L_{\parallel} is connected with *c*-crystal axis, $L_{\parallel} + 2L_{\perp} = 1$) and the filling factor, f . The shape factor takes values from zero for the cylinder, to unity for the slab [17]. The filling factor, f , represents the fraction of the total sample volume occupied by ellipsoids; its value ranges from 0 for individual particles to 1 for dense aggregates.

RESULTS

In the present work, the most attention is given to changes taking place in zinc oxide. EPR signals were not detected in the initial ZnO powders. MT of the pure ZnO and mixture ZnO – TiO₂ resulted in the initiation of a set of EPR signals (Fig. 2, Table 1), typical for

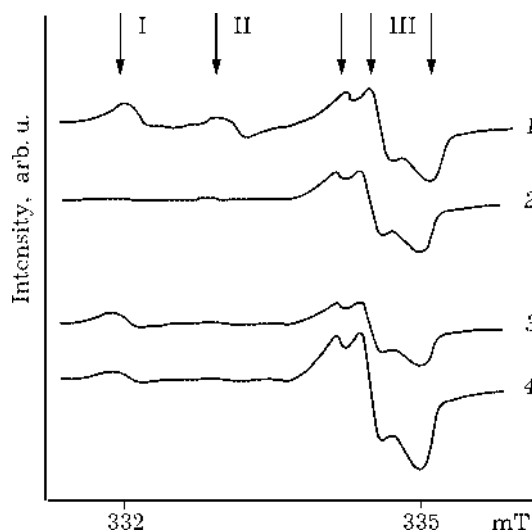


Fig. 2. EPR spectra initiated in ZnO by MT of ZnO (1, 2) and ZnO - TiO₂ (3, 4) samples. t_{MT} , min: 30 (1, 4), 300 (2), and 5 (3).

various electron-hole centres in zinc oxide. In the Table 1, the parameters of a spin-Hamiltonian of these centres are given as well as the types of the centres which were identified by comparison of the obtained results with published data for single crystal samples [18–21]. In the initial TiO₂, a number of small asymmetric EPR signals with $g \sim 2$ –1.94 were registered. Since these signals did not practically overlap with analyzed EPR signals I–III in mechanically treated ZnO, they will not be taken into consideration in the present work. The change in the intensity of EPR signals from centres I, II and III in ZnO and ZnO - TiO₂ samples depending on the MT duration is shown in Fig. 3. The EPR signal from centres II in samples ZnO - TiO₂ was practically absent. Moreover, in these samples, EPR signal from

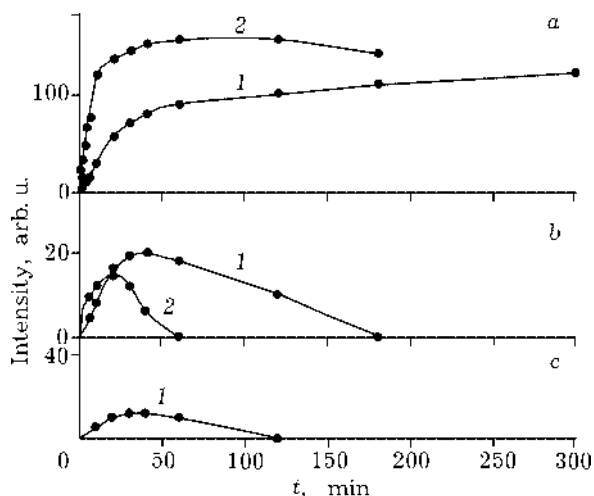


Fig. 3. Change of the intensities of EPR signals III (a), I (b) and II (c) in ZnO vs. duration of MT of ZnO (1) and ZnO - TiO₂ (2) samples.

the SDS centres V observed in mechanically treated samples of pure ZnO [12] was absent.

At the initial stage, the intensity of EPR signals from centres I, II and III is proportional to t_{MT} (see Fig. 3). The infringement of such proportionality with increasing t_{MT} indicates the end of the initial stage of MT. The times of the initial stage, t_1 , are different for the system ZnO - TiO₂ ($t_1 \gg 10$ min) and ZnO ($t_1 \gg 30$ min). At this stage, the values of dI_{III}/dt for ZnO - TiO₂ and ZnO samples are proportional to the microhardness constants for TiO₂ and ZnO, respectively. This means that, during MT of the ZnO - TiO₂ powder mixtures having different microhardness of components, the rate of defect formation in the softer ZnO is proportional to the ratio of microhardnesses of the components: H_{TiO_2}/H_{ZnO} .

Figure 4 presents changes in intensity of the signals I, II, and III (in ZnO samples at

TABLE 1

Values of obtained parameters of EPR signals in the MT zinc oxide powder and parameters of signals of defects obtained in studies of single crystals

| Signal | Values of g -factors obtained in this work | Centre | Values of g -factors obtained on single crystals | Ref. |
|--------|--|----------------------|---|------|
| I | $g_{\perp} = 2.0190$, $g_{\parallel} < g_{\perp}$ | $V_{Zn}^{-}:Zn_i^0$ | $g_{xx} = 2.0185$, $g_{yy} = 2.0188$, $g_{zz} = 2.0040$ | [18] |
| II | $g_{\perp} = 2.0130$, $g_{\parallel} = 2.0140$ | V_{Zn}^{-} | $g_{\perp} = 2.0128$, $g_{\parallel} = 2.0142$ | [19] |
| III | $g_1 = 2.0075$, $g_2 = 2.0060$, $g_3 = 2.0015$ | $(V_{Zn}^{-})_2^{-}$ | $g_{xx} = 2.0077$, $g_{yy} = 2.0010$, $g_{zz} = 2.0059$ | [18] |
| IV | $g_{\perp} = 1.9965$, $g_{\parallel} = 1.9950$ | V_O^{+} | $g_{\perp} = 1.9963$, $g_{\parallel} = 1.9948$ | [20] |
| V | $g = 1.964$ | SDS | $g \gg 1.96$ | [21] |

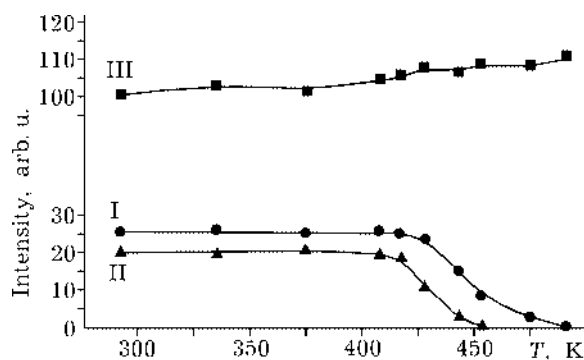


Fig. 4. Change of the intensities of EPR signals I, II and III in ZnO sample ($t_{MT} = 30$ min) vs. annealing temperature.

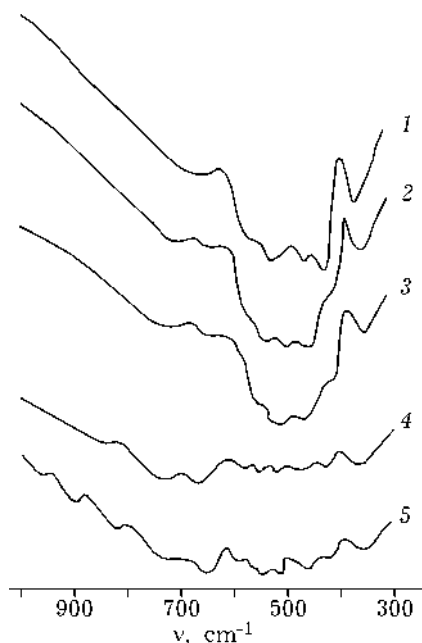


Fig. 5. IR absorption spectra of ZnO - TiO₂ powders subjected to MT: 1 - the initial mixture; 2-5 - treated for 3 min (1), 30 (3), 90 (4) and 180 min (5).

$t_{MT} \gg 30$ min) as a function on the annealing temperature, T_{an} , ($t_{an} = 3$ min). Beginning from $T_{an} = 428$ K, a decrease of the signal II was observed. Signal II practically disappeared after treatment at $T_{an} = 453$ K. A decrease of the signal I was observed beginning from $T_{an} \sim 443$ K; it disappeared after treatment at $T_{an} = 493$ K. These data allow us to interpret the centres responsible for signal III as the most thermally stable formations and the centres responsible for signal II as the least stable ones. According to our rough guess (using the data given at Fig. 4), activation energy, E , for the annealing of centres II is $E_{II} \sim 1.15$ eV, while for the centres of I type $E_I \sim 1.3$ eV (for the centres III, E is even higher).

IR spectra of the initial and mechanically treated samples of the ZnO - TiO₂ system are shown in Fig. 5. In these spectra, absorption bands characteristic of both ZnO and TiO₂ are present (Table 2). The identification of these bands by the TADC indicates the formation of a wide morphological set of particles in the given disperse system [13]. For instance, absorption bands in the range $440-550$ cm⁻¹ correspond to needle-like ZnO particles with a shape parameter (l/d , where l is the length of a particle, d is its diameter) ranging from 1 to 4 ($n_5 \gg 510$ cm⁻¹ for $l/d = 1$, $n_6 \gg 540$ cm⁻¹ and $n_4 \gg 490$ cm⁻¹ for $l/d = 2$, $n_3 \gg 440$ cm⁻¹ for $l/d = 4$). The intensity of these bands is proportional to the concentration of particles of certain shape.

As the grinding time increases, the morphological set of particles changes. Increases in the intensities of the bands at n_4 , n_5 and n_6 indicate increases in the content of ZnO parti-

TABLE 2

The frequencies of IR absorption bands in the mechanically treated system ZnO - TiO₂, cm⁻¹

| Time of mechanical treatment, min | ZnO | | | | | | | TiO ₂ | | Interaction products | | |
|-----------------------------------|-------|-------|-------|-------|-------|-------|-------|------------------|-------|----------------------|----------|----------|
| | n_1 | n_2 | n_3 | n_4 | n_5 | n_6 | n_7 | n_8 | n_9 | n_{10} | n_{11} | n_{12} |
| 0 | 350 | 420 | 440 | | 510 | 550 | | 640 | | | | |
| 3 | 350 | 415 | 450 | 490 | 515 | 545 | | 640 | 710 | | | |
| 30 | 350 | 410 | 457 | | 510 | 540 | | 630 | 725 | | | |
| 90 | 350 | 410 | 455 | | 510 | 545 | 575 | 635 | 725 | 820 | | |
| 180 | 350 | 410 | 450 | | 515 | 540 | 570 | 635 | 720 | 820 | 900 | 940 |

cles with the shape parameter 1 and 2 in samples. The appearance of the band at $n_7 \approx 575 \text{ cm}^{-1}$ after $t_{\text{MT}} = 90\text{--}180 \text{ min}$ indicates that plate-like ZnO formations appear. The absorption band at $n_8 \approx 640 \text{ cm}^{-1}$ corresponds to equiaxial TiO_2 particles. A change in its intensity with increasing time of MT reflects the dynamics of a rise in the content of such particles in samples. The appearance of the band at $n_9 \approx 720 \text{ cm}^{-1}$ and an increase in its intensity at the time of MT $t_{\text{MT}} = 180 \text{ min}$ are caused by the formation of plate-like TiO_2 particles or their flat aggregates. Beginning from $t_{\text{MT}} \approx 30 \text{ min}$, the weakening of the intensity of the whole IR absorption spectrum is observed. At $t_{\text{MT}} = 90\text{--}180 \text{ min}$, it consists of a set of weak bands (see Fig. 5). This points to a change in the morphology of particles and their aggregation as well as to interphase interaction processes. The appearance of absorption bands at n_{10} , n_{11} и n_{12} can be attributed to the formation of a new phase. Note, however, that X-ray studies did not detect new phases in these samples.

Analysis of experimental results

With the help of the EPR method, it has been shown earlier [12], that as t_{MT} of ZnO increases, the transition from the perfect lattice in the initial specimen ($\text{Zn}_{\text{lat}}^{2+}$) through the complexes zinc vacancy – interstitial zinc ($\text{V}_{\text{Zn}}^- : \text{Zn}_i^0$ – centre I) [18], zinc monovacancies (V_{Zn}^- – centre II) [19] to two-vacancy complexes ($(\text{V}_{\text{Zn}}^-)_2$ – centre III) [18] takes place (see Table 1). Then the further transformation of vacancies in the oxygen sublattice ((V_{O}^+) – centre IV) [20] towards defects consolidation into the so-called shallow donor states ((SDS) – centre V) occurs [21] (see Table 1). The disappearance of some centres and appearance of others depends on t_{MT} and indicates the differences in their annealing activation energy. Thus, paramagnetic centres of types I–V could serve as probes for mechanothermal processes in systems containing zinc oxide.

The $t_{\text{MT}} < t_1$ stage

Significant qualitative differences in the shapes of EPR spectra which were registered

in ZnO at the beginning of the MT of the ZnO and ZnO – TiO_2 samples provide evidence that the destruction-deformation processes do not represent the development of a single crack or a slip band in an individual ZnO particle; they are not the result of the accumulation of such acts of destruction. In this case, the spectra in the ZnO and ZnO – TiO_2 samples should be the same. The differences in the EPR spectra show that the local (in the ZnO particle) collective processes take place. It is possible to suppose that, at every specific moment of the loading time, the individual ZnO particles that are in “states the most optimal for destruction”, are subjected to this process in full measure (Fig. 6, *a* and *b*). In the particles, the intensive defect formation takes place, and they play the role of sources of heat release. The number of such «states» for ZnO powders depends on the mechanical characteristics of the components in the disperse systems.

The qualitative difference of EPR signals shape in ZnO and ZnO – TiO_2 samples de-

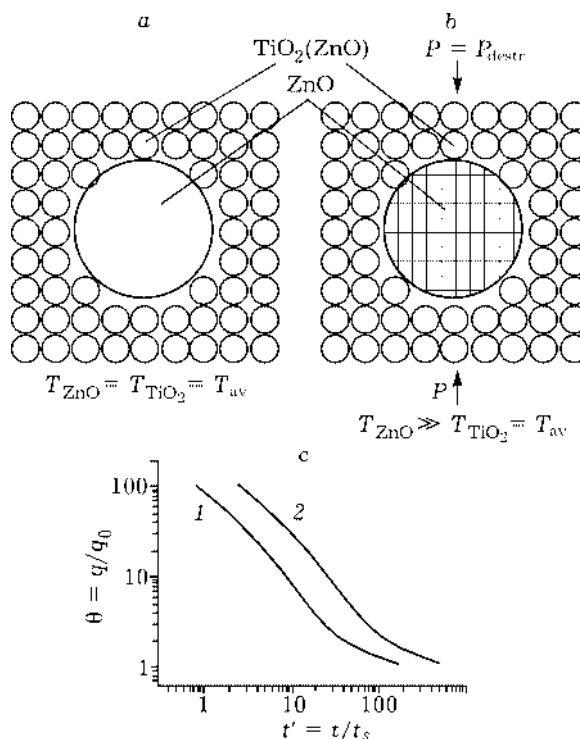


Fig. 6. Destruction model of an individual ZnO particle in an environment of other particles: *a* – before destruction; *b* – at the moment of destruction; *c* – kinetics of changes of temperature excitation [19] in ZnO particle surrounded by the ZnO (1) or TiO_2 (2) particles.

depends on the thermal conductivity of ZnO and the TiO₂ additive and they are similar to those observed under heat treatment. This allows us to connect the difference with the development of the thermal processes and the effect of spike annealing of defects in individual ZnO particles during the MT. The rate of the change of the particle's energy density can be estimated from the heat transfer equations using a model of passive cooling [22]. Let us use calculations made in [22] for the case of decay of the local energy excitation with time:

$$q = Q/(4\pi c t)^{3/2} \exp(-r^2/(4ct)) \quad (1)$$

where Q is the heat released at the moment $t = 0$ at the point $r = 0$, c is the coefficient of thermal conductivity. With the assumption that "thermoactive" particles in the environment are formed by TiO₂ (specimens of ZnO – TiO₂) and ZnO (specimens of ZnO) particles, expression (1) enables us to describe qualitatively their temperature regimes (see Fig. 6, c). It is easy to show that the duration, τ , of the thermal spike of the particle is inversely proportional to the thermal conductivity (c) of its environment, *i. e.* $\tau \sim 1/c$. From this point of view, the smaller duration of the annealing heat spike must be observed in the ZnO specimens and the larger duration in the ZnO – TiO₂ specimens (see Fig. 6, c).

It should be noted that, if the EPR data reflect the kinetics of formation of vacancy centres, the IR spectrometry data indicate the fact that, in samples, at $t_{MT} < t_1$, macroscopic changes reflecting the initial processes of interphase interaction take place. In our opinion, an increase in the concentration of equiaxial (spherical) TiO₂ formations is connected with the enveloping process of small equiaxial ZnO particles by a TiO₂ layer. It is not improbable that, in the formation of the surface layer, amorphous TiO₂, the presence of which is registered by X-ray methods in the starting mixtures, takes part. Its concentration drops as t_{MT} increases up to 30 min by about 2.5 times.

The $t_{MT} > t_1$. Thermoaccumulation processes

At the initial stage of processing, the rate of the T_{av} increase for a sample is determined

to a high extent by the rate of defect formation, *i. e.*, it is possible to consider that $T_{av}(t_{MT}) \sim (dI_{III}/dt)t$. Within the framework of the present investigation, $dI_{ZnO-TiO_2}/dI_{ZnO} \sim H_{TiO_2}/H_{ZnO}$. This implies that an interval of time required for the ZnO – TiO₂ sample to achieve threshold temperatures at which the annealing of registered defects begins (centres I) is approximately H_{TiO_2}/H_{ZnO} times shorter than that for the pure ZnO samples. The qualitatively second stage of the MT, in which the lower-temperature but more prolonged annealing takes place, begins here. At this stage, the achieved thermal effect exerts an essential influence on defect formation. Defects formed at the first stage of the MT are annealed first.

An increase in the time of the MT ($t_{MT} > t_1$) leads to a change in the shape of the signals registered (see Fig. 2) and to a change in the ratio of the intensities of different centers (see Fig. 3). The EPR signal from centres II disappears first. In ZnO samples, this signal disappears after $t_{MT} \gg 120$ min. Then there is a change in the intensity of signals from the centres I. In ZnO – TiO₂ samples, this signal disappears after $t_{MT} \gg 60$ min and, in ZnO samples, after $t_{MT} \gg 180$ min. The intensity of the most stable signal from centres III attains the maximal value in ZnO – TiO₂ samples after $t_{MT} \gg 120$ min (in ZnO samples at $t_{MT} \gg 300$ min), and then its weakening is observed (see Fig. 3). The obtained results allowed us to construct the diagram of growth of the average temperatures of ZnO – TiO₂ and ZnO samples with increasing t_{MT} (Fig. 7).

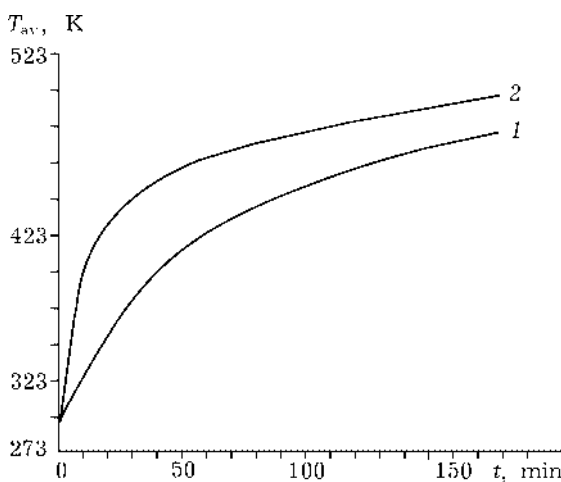


Fig. 7. Change of the average temperature in ZnO (1) and ZnO – TiO₂ (2) samples *vs.* duration of MT.

The attainment of the saturation and a subsequent weakening of signal III in ZnO – TiO₂ samples ($t_{MT} \gg 60\text{--}120$ min) are most likely connected with the beginning of the interphase reaction between ZnO and TiO₂. As a result of this interaction, the signal from SDS is absent but it is registered in pure ZnO samples. According to the data of [23], such a situation takes place when different impurities (in this case, Ti ions) find their way into the surface layers of ZnO particles, which is substantiated by the IR spectroscopy data presented above.

DISCUSSION

The following simplified scheme of evolution of the fine defective structure in the ZnO – TiO₂ system in different stages of the continuous MT becomes evident.

At the initial stage, which can be considered as pure grinding, the MT forms a rather simple vacancy structure in the fracture zone of a less strong component of the mixture, namely, on ZnO particles. As a result of the pulse destruction of ZnO particles, heat evolves. As this takes place, “the local pulse annealing” of formed defects occurs. The annealing effect is determined by the activation energy of annealing of defects and by the time of the thermal pulse. The time of the thermal pulse is defined by the thermal conductivity of the environment of the particle. Low-energy defects are more chemically active, and, in view of their surface localization, can take an active part in the formation of cohesive contacts with particle of another phase.

At this stage of MT, the accumulation of defects in the sample occurs mainly due to grinding of particles that have not broken down yet. One should bear in mind that particles formed at the initial stages of MT do not disintegrate further up to the period of relative equalization of the average particle size in the sample. These small particles, however, participate in the formation of the environment of disintegrating larger particles, find themselves in a heat field induced by the latter particles, and contact continuously with other particles and milling bodies. This favours the modification of their surface defective struc-

ture due to pure mechanical interaction (less radical than at direct fracture) and under the influence of the heat, which evolves in the process. However, relatively low-temperature and short-time effects do not exert a significant influence on the formed defective structure.

Thus, we can draw the conclusion that, during mechanothermal annealing, the defective structure of the new-formed particle becomes more perfect and more complex. As the structure becomes more complex, defect associates whose activation energy of annealing exceeds those of their elementary (point) defects, accumulate first.

Radical changes begin to manifest themselves at the second stage ($t_{MT} > t_1$) when the sample attains the average temperature which is sufficient for complete annealing of low-temperature defects in a continuous regime and favours the efficient generation of defects (associates) with higher energy. During long MT, both the equilibrium temperature of the sample and mechanical stresses generated must set the type of the defective structure formed in the sample. From the viewpoint of an interphase interaction of the type $\text{ZnO} + \text{TiO}_2 \rightarrow \text{ZnTiO}_3$, the accumulation of the associates of defects by individual phases is a necessary prerequisite for the interaction to proceed by the pure diffusion mechanism at rather low temperatures [23]. The results presented above show that T_{av} of the sample attains significant values even when not high-energy conditions of MT are used. It is well to bear in mind that an increase in T_{av} favours the widening of thermal pulses formed during mechanical action, thus increasing their reactive influence.

CONCLUSIONS

The results obtained enable us to propose the two-stage scheme of development of thermal processes in the considered disperse systems and establish their role in the formation of resulting defective structure. At the first stage of the MT, the collective destruction of individual particles is observed. The formed defects (within a single particle) are located in a high-temperature field, which is created by set of the ultrahigh-temperature and very short

spikes. Thus, the annealing effect is described by a kinetic curve of thermal excitation of the whole particle. The character of the kinetic curve is determined by the thermal conductivity of the environment of the particle. At the first stage, the annealing effect will manifest itself more strongly during MT of the systems containing the additives with lower heat conductivity.

The second stage of processing is connected with the development of annealing effects caused by heat accumulation processes by the whole sample. Such processes occur at considerably lower temperatures than those of the first stage, but their duration (especially upon achievement of equilibrium conditions) becomes proportional to t_{MT} . Since the rate of defect formation in the ZnO – TiO₂ system is determined by the microhardness of TiO₂ particles, which is about 5 times larger than that of ZnO, then the rate of increase of T_{av} in this sample at the first stage of the MT is about 5 times larger than that in the ZnO sample. Thus, annealing effects connected with the threshold processes of heat accumulation manifest themselves in the ZnO – TiO₂ system much earlier than in the ZnO system. During MT, the annealing processes favour the formation and accumulation of a set of associates of simple defects that accelerate diffusion processes in components of the mixtures. Thus, the accumulation of associates of defects in the sample and a significant rise in the average temperature of the sample are major factors determining the progress of a mechanochemical reaction of the type $ZnO + TiO_2 \rightarrow ZnTiO_3$.

REFERENCES

- 1 G. Heinicke, *Tribochemistry*, Akademie-Verlag, Berlin, 1984.
- 2 E. G. Avvakumov, *Mekhanicheskiye metody aktivatsii khimicheskikh protsessov*, Novosibirsk, Nauka, 1986.
- 3 F. P. Bowden and P. A. Persson, *Proc. Roy. Soc.*, A260 (1961) 433.
- 4 K. B. Broberg, *Cracks and Fracture*, Academic Press, San Diego *etc.*, 1999.
- 5 F. Urakayev, *Izv. SO AN SSSR. Ser. khim.*, 3 (1978) 5.
- 6 R. Weichert and K. Schonert, *J. Mech. Phys. Solids*, 26 (1978) 151.
- 7 P. G. Fox and J. Soria-Ruiz, *Proc. Roy. Soc.*, A317 (1970) 79.
- 8 V. V. Boldyrev, *Kinetics and Catalysis*, 13 (1972) 1414.
- 9 N. Z. Lyahov, *Baniche Listy (Mimoriadne cislo)*, VEDA, Bratislava, 1984, s. 40–48.
- 10 Junmin Xue, John Wang and Dongmei Wan, *J. Am. Cer. Soc.*, 83 (2000) 232.
- 11 O. Abe and Y. Suzuki, *Mater. Sci. Forum*, 225–227 (1996) 563.
- 12 N. G. Kakazey, T. V. Sreckovic and M. M. Ristic, *J. Mater. Sci.*, 32 (1997) 4619.
- 13 M. G. Kakazey, V. A. Melnikova, T. Sreckovic *et al.*, *J. Mater. Sci.*, 34 (1999) 1691.
- 14 N. G. Kakazey, L. A. Klockov, I. I. Timofeeva *et al.*, *Cryst. Res. Technol.*, 34 (1999) 859.
- 15 G. V. Samsonov (Ed.), *The Oxide Handbook*, IFI/Plenum, New York *etc.*, 1982.
- 16 S. Hayashi, N. Nakamori and H. Kanamori, *J. Phys. Soc. Japan*, 46, 176 (1979).
- 17 C. J. Serna and J. E. Ingleasias, *J. Phys.*, C20 (1987) 472.
- 18 B. Schallenberger, A. Hausmann, *Z. Physik*, B23 (1976) 177.
- 19 J. M. Smith and W. E. Vehse, *Phys. Lett.*, 31A (1970) 147.
- 20 V. A. Nikitenko, *Zhurn. prikl. khimii*, 57 (1992) 367.
- 21 R. Shone, *Chem. Ing. Techn.*, 41 (1969) 282.
- 22 A. B. Roitsin, V. M. Mayevsky, *Radiospektroskopiya poverkhnosti tverdykh tel*, Naukova dumka, Kiev, 1992, p. 268.
- 23 F. A. Kroger, *The Chemistry of Imperfect Crystals*, Philips Research laboratories, Eindhoven, The Netherlands, North-Holland Publishing Company, Amsterdam, 1964.